PERGAMON

Atmospheric Environment 36 (2002) 2853–2865

ATMOSPHERIC ENVIRONMENT

www.elsevier.com/locate/atmosenv

Daily cycles in urban aerosols observed in Florence (Italy) by means of an automatic 532–1064 nm LIDAR

Massimo Del Guasta

IROE CNR, Via Panciatichi 64, 50127 Firenze, Italy

Received 10 September 2001; received in revised form 12 December 2001; accepted 9 January 2002

Abstract

An unattended light detection and ranging (LIDAR) operating at 532–1064 nm was used for the continuous monitoring of the planetary boundary layer (PBL) of Florence (Italy). This was the first time that such a well-established remote-sensing technique has been used in Italy as a monitoring tool for the long-term study of urban aerosols: time–height–backscatter plots were used for the interpretation of the PBL dynamics and the vertical distribution of the aerosols, while the aerosol backscatter and its wavelength dependency were used to estimate the mass concentration and the median size of the aerosols 40 m above the ground. The marked wavelength dependency shown by traffic-related aerosols permitted a distinction between fresh urban and background/rural aerosols. In summer, the aerosol mass concentration and the backscatter Ångström coefficient showed well-defined and very similar daily cycles with a marked peak in the morning and shallow minima in the afternoon. The morning mass peak was produced by small particles (0.05–0.1 μm mode diameter), while there was a prevalence of larger particles in the afternoon. The observed cycles were the result of a coupling between the traffic cycle and the daily surface-wind cycle: fresh urban aerosols produced in town were advected above the LIDAR in the morning by the persisting nighttime breeze. The reversal of the breeze in the late morning was responsible for the low-aerosol concentration observed in the afternoon, when rural air containing a low concentration of relatively large aerosols reached the LIDAR, and dilution of urban aerosol through turbulent mixing occurred. By assuming an exponential decay of aerosol concentration with height, the LIDAR-derived scaling height showed a minimum (100–200 m) in the afternoon, in coincidence with the advection of air from the suburbs. The mass concentration variations were found to be strictly correlated with traffic at night and in the early morning, when the local breeze brought the urban plume above the LIDAR site. The high temporal resolution of the LIDAR made it possible to follow the aerosol mass variations with a 5 min resolution, fast enough to follow the rapid aerosol peak evolution in the morning: the peak mass concentration was 5–10 times larger than during the rest of the day, suggesting the inadequacy of the daily averaged aerosol mass measurements carried out at present by the local authorities. © 2002 Published by Elsevier Science Ltd.

Keywords: LIDAR; Urban aerosol; Particulate; Remote sensing; PBL

1. Introduction

Light detection and ranging (LIDAR) systems are valuable tools for planetary boundary layer (PBL) studies. The high temporal and spatial resolution of elastic-backscatter LIDARs makes it possible to obtain real-time "snapshots" of the PBL in the form of time–height–backscatter plots. These plots can be used to interpret ground-based pollution measurements in terms of PBL dynamics. LIDARs operating at 532–1064 nm, which are quite popular because of the reliability of Nd–YAG laser sources, could be configured for unmanned operations, and have been often used for investigating the urban PBL (e.g. Devara et al., 1994; Menut et al., 1997). The high resolution of LIDAR measurements is balanced by scarce accuracy

E-mail address: dguasta@iroe.fi.cnr.it (M. Del Guasta).

1352-2310/02/$ - see front matter
PII: S1352-2310(02)00136-X

when the signal is inverted, in terms of aerosol quantities of current use (e.g. aerosol mass concentration). This problem is partly due to the uncertainties involved in the conversion of the raw LIDAR signal to calibrated backscatter profiles, and partly to an ignorance of the aerosol characteristics involved in converting backscatter profiles into microphysical quantities. These quantities (complex refractive index, size distribution shape, etc.) are highly variable in the PBL. In situ instrumentation and/or Raman LIDARs (Di Girolamo et al., 1999) have been used in order to reduce the uncertainty of LIDAR-derived microphysical quantities in urban areas, but at present these techniques can be afforded only in short-term campaigns. Aerosol mass concentration is one of the few aerosol quantities of general interest that could be retrieved from elastic-backscatter LIDAR data with acceptable accuracy: several works have shown that, in many cases, aerosol mass could be derived with an accuracy of 20–30% from LIDAR data also in the absence of ancillary information about the aerosols (Kent, 1978; Del Guasta and Marini, 2000). This is due to a rough proportionality that exists between the accumulation-mode aerosol mass and the scattering cross section for visible light (Willeke and Baron, 1993).

The wavelength dependency of LIDAR backscatter between 532 and 1064 nm can also be used to estimate the aerosol size. The uncertainties involved in this process are unacceptable for a quantitative measurement of the aerosol median size in the urban atmosphere (Del Guasta and Marini, 2000); nevertheless, it is possible by this means to distinguish between the very fine (and hazardous) primary aerosols produced by traffic and the larger aerosols of background or rural origin, and to use this difference as a finger print of the origin of the air mass probed by LIDAR. In this paper, a summary of summer data from several years of the unattended operation of a 532–1064 nm LIDAR is presented. The results are discussed in terms of PBL dynamics and pollution sources.

2. Methods

2.1. The LIDAR system

In the PBL LIDAR system used in Florence an Nd–YAG laser source (532 + 1064 nm) was used, firing pulses of 15 ns duration with a 20 Hz repetition rate. The output energies were ~3 mJ at 1064 nm and 0.5 mJ at 532 nm. The output energies were automatically adjusted via computer in order to prevent the detector saturation. The output energies of the laser were measured shot-by-shot by two solid-state energy meters developed at IROE (Del Guasta and Venturi, 1998). The laser beam, coaxial with the telescope axis, was sent vertically into the atmosphere through a slanted waterproof Pyrex window. The backscattered light was collected by a 22 cm telescope and split into two beams (visible and infrared) by means of a dichroic mirror. Two independent field stops were used for the two wavelengths, determining a field of view of a 2 mrad full angle, corresponding to a full overlap of telescope and laser beam at about 30 m above the ground. The two light beams were analyzed by means of two narrow band-pass interference filters (0.15 nm bandwidth at 532 nm, and 1 nm at 1064 nm) before reaching the detectors: a PMT at 532, and a Peltier-cooled avalanche photodiode (EG&G C30956E) at 1064 nm. The signal acquisition was performed by a 9304 LeCroy digital oscilloscope, communicating with the PC. The PC fired a burst of 200 laser shots every 5 min. The height resolution was 3 m. The laser energies and meteorological data were acquired by means of a National Instruments multifunction board. The relative humidity (RH) was measured at the LIDAR site by a Vaisala Humicap. The LIDAR was fired automatically, 24 h day^{-1} and almost continuously from 1996 to 2000.

2.2. LIDAR data processing

The LIDAR signal can be expressed as (e.g. Collis and Russel, 1976):

$$V_\lambda(z) = k_\lambda E_{0,\lambda} \frac{1}{z^2} (\beta_{a,\lambda}(z) + \beta_{m,\lambda}(z)) e^{-2\int_0^z (\sigma_{a,\lambda}(z') + \sigma_{m,\lambda}(z'))\,dz'}, \quad (1)$$

where $V(z)$ is the signal received from the altitude z, k is the LIDAR constant, $E_{0,\lambda}$ is the pulse energy, β is the volume backscatter (m^{-1} sr^{-1}), and σ is the extinction coefficient (m^{-1}). The suffixes "a" and "m" refer to the aerosol and molecular components of the atmospheric backscatter and extinction. There are two similar equations for the two wavelengths λ (532 and 1064 nm).

The LIDAR signals were acquired up to 1500 m height. The raw signals at the two wavelengths were normalized to the laser energies, noise-subtracted, and square-range corrected (Measures, 1988). At this point, the conversion of LIDAR data to aerosol mass required a normalization of the profiles into backscatter units. In this study, where the aerosol close to the ground was the main topic, the laser energies were small, in order to prevent detector saturation in the lowest part of the signal. Under these conditions, the 532 and 1064 nm LIDAR signals from the low PBL (between 40 and 300–500 m above ground) were strong enough to show an S/N ratio larger than ten even in the cleanest air conditions. However, the signal from the clear, free troposphere was very weak, and it was impossible to normalize the LIDAR profile to the molecular atmosphere well above the PBL. No procedure for the extinction correction of the signal, such as the

widespread Klett's method (Klett, 1981) was thus applied. LIDAR profiles were therefore normalized to the molecular backscatter in the "cleanest" profiles of a monthly data set. For this purpose, the 532–1064 nm LIDAR data at 40 m above the ground were plotted in a scatter plot. The minimum signals at the two wavelengths, corresponding to the cleanest air recorded during that period, were normalized to the Rayleigh backscatter at both wavelengths. The same normalization constant was used for all the other LIDAR signals. On the ground, $\beta_{m,\lambda}(z)$ was computed from T and P using the following equation (Penndorf, 1957):

$$\beta_{m,\lambda}(0)_{(m^{-1}\,sr^{-1})} = 3.7367 \times 10^{-8} \frac{P(\text{mbar})}{(T[\text{K}])(\lambda[\mu\text{m}])^4}, \quad (2)$$

$\beta_{m,\lambda}(0)$ is $10^{-7}\,m^{-1}\,sr^{-1}$ at 1064 nm and $1.6 \times 10^{-6}\,m^{-1}\,sr^{-1}$ at 532 nm with 5% uncertainty. This procedure is reliable if several conditions are controlled: the LIDAR window must always be clean; the laser energy must be precisely known; and the system constant k_λ (a function of optics transmission and detector efficiencies) must be kept constant. To this end, the 1064 nm detectors (both for signal and energy detection) were thermally stabilized. Water condensation and dust deposits on the LIDAR window were removed using constant ventilation and an automatic car wiper, respectively. The relative uncertainty of the factor k_λ at both the wavelengths was estimated to be 5–10%. The overall error in the aerosol backscatter arose from many causes, among which are the uncertainty of k_λ, errors in the background and noise-subtraction, and nonlinearities in the detecting electronics. The overall error in the aerosol backscatter could not be precisely computed, but was estimated to be 10–15% at 532 nm and 20–25% at 1064 nm.

After normalization and square-range correction, the LIDAR signal can be expressed by

$$V'_\lambda(z) = [\beta_{a,\lambda}(z) + \beta_{m,\lambda}(z)]e^{-2\int_0^z(\sigma_{a,\lambda}(z')+\sigma_{m,\lambda}(z'))\,dz'}. \quad (3)$$

When the measurement of the aerosol mass close to the ground is the main goal of our LIDAR research, the exponential term caused by extinction can be considered unitary, as the normalized LIDAR data becomes coincident with the total volume backscatter coefficient $[\beta_{a,\lambda}(z) + \beta_{m,\lambda}(z)]$. Mie simulations carried out on a large variety of tropospheric aerosol models (Ackermann, 1998; Del Guasta and Marini, 2000) and in situ measurements (Anderson et al., 2000) showed that the ratio $\sigma_{a,\lambda}/\beta_{a,\lambda}$ is smaller than 100 sr: thus, the exponential term in Eq. (3) differs from unity by $< 10\%$ up to a height of at least 50 m, even with the heaviest urban aerosol loadings observed in Florence ($\beta_{a,532}(50) \approx 2 \times 10^{-5}\,m^{-1}\,sr^{-1}$). The approximation fails in the case of fog (in which case, $\sigma_{a,\lambda}/\beta_{a,\lambda} \cong 15 - 20$ sr (Pinnick et al., 1983; Ackermann, 1998)) when $\beta_{a,532}(50) > 10^{-4}\,m^{-1}\,sr^{-1}$. In case of fog, however, the 532–1064 nm LIDAR data cannot be inverted in order to retrieve the aerosol mass (Del Guasta and Marini, 2000). In this work, the aerosol mass at a height of 40 m above the ground was computed quantitatively, disregarding the aerosol extinction. By disregarding extinction, the processed LIDAR data is simply

$$V'_\lambda(z) \approx [\beta_{a,\lambda}(z) + \beta_{m,\lambda}(z)] \quad (4)$$

Subtraction of the molecular, volume backscatter $\beta_{m,\lambda}(z)$ from Eq. (4) leads to the absolute aerosol volume backscatter $\beta_{a,\lambda}(z)$; thus, $\beta_{a,\lambda}(z)$ were obtained from each LIDAR measurement at the selected level of 40 m above the ground.

The backscatter Ångström coefficient was computed by

$$\alpha(z) = \frac{\ln(\beta_{a,532}(z)/\beta_{a,1064}(z))}{\ln(2)}. \quad (5)$$

2.3. Estimation of the aerosol mass concentration

The backscatter Ångström coefficient α is a complex function of the aerosol composition and size distribution, which are functions of the dry particle composition and of the environmental RH. As a first step, by assuming that the LIDAR backscatter in the urban PBL is dominated by the accumulation-mode aerosols produced by combustion, the aerosol Ångström coefficient (α) was calculated for populations of lognormally distributed aerosols showing a wide range of dry mode radius ($0.02\,\mu m < r_m < 1\,\mu m$) and distribution widths ($1.4 < s < 2.2$) (Del Guasta and Marini, 2000). In these simulations, the aerosol refractive index and mode radius of the "wet" aerosol (in equilibrium with RH) were calculated for different RH values ($50\% < RH < 95\%$) by assuming the thermodynamic equilibrium and with ammonium sulphate $(NH_4)_2SO_4$ as the main soluble component of the dry aerosol. In the simulations, we considered the presence of black carbon to account for an imaginary part of the refractive index as tabled by Shettle and Fenn (1979) for their urban aerosol model. The possible presence of insoluble material making up 0–50% of the dry mass was also considered as a possible source of uncertainty.

After an exploratory survey, the urban aerosol mass was found to be the only aerosol quantity measurable with a reasonable uncertainty from this type of LIDAR data. Other quantities, such as aerosol size and number concentration, were affected by uncertainties that were often larger than 50%.

For each log-normal aerosol population in equilibrium with the environmental humidity and with a mass concentration $M_{wet}(kg\,m^{-3})$, the mass specific volume

backscatter

$$CM_{532} = \frac{M_{wet}}{\beta_{a,532}} \quad (6)$$

was calculated and plotted against RH and α. This quantity made it possible to compute the "wet" aerosol mass concentration from 532 to 1064 nm LIDAR data. The range assumed by CM_{532} values at fixed RH and α was assumed to be the uncertainty range of CM_{532} due to our ignorance of the aerosol properties. In this process, a possible experimental uncertainty of 0.4 for α (corresponding to the backscatter uncertainties), and 1% in RH were considered.

This process is valid when the coarse aerosol contribution to backscatter is negligible when compared to the contribution from the accumulation aerosols. In most cases (including the urban environment), this hypothesis is rarely satisfied, and assuming a monomodal distribution in the aerosol simulations can lead to mass underestimations of up to −30% (Del Guasta and Marini, 2000). A continuous monitoring of the coarse aerosol size spectrum is actually possible with optical particle sizers, and this information could make it possible to reduce the CM_{532} error due to coarse particles. Unfortunately, this facility is not yet available at our LIDAR site, and for this reason we used the aerosol size spectra available from the literature in order to estimate the coarse aerosol error. To this end, the simulations performed for monomodal aerosols were repeated, and included the presence of coarse aerosols of variable nature (NaCl, $(NH_4)_2SO_4$, sulphuric acid, rural dust, etc.) at different RH and for the different, actual size distributions of urban aerosols available from the literature (Del Guasta and Marini, 2000). This process made it possible to estimate the error in mass that occurs when fitting the 532–1064 nm LIDAR data with a monomodal aerosol distribution. This error was used to modify the CM_{532} uncertainty bar as obtained with monomodal distributions for fixed (RH, α) pairs.

A minimum and a maximum CM_{532} were thus obtained as functions of (RH, α). In this way, it was possible to compute a range of CM_{532} on the basis of experimental (RH, α) pairs. Lastly, the minimum and maximum aerosol mass concentrations (M_{wet}) were computed by using the simple relations:

$$M_{wet\,max} = CM_{532\,max} \times (\beta_{a,532} + \Delta\beta_{a,532}), \quad (7)$$

$$M_{wet\,min} = CM_{532\,min} \times (\beta_{a,532} - \Delta\beta_{a,532}), \quad (8)$$

where $\Delta\beta_{a,532}$ is the absolute, experimental backscatter error.

This calculation was performed in this work at the minimum LIDAR valid height (40 m) in order to use the LIDAR data in comparison with the ground-based pollution data.

The dry mass M_{dry} was calculated from M_{wet} by simulating the hygroscopic de-growth of the aerosol. This process is well known only for pure solutes, and is affected by several uncertainties in real aerosols due to the presence of organic compounds (Pradeep et al., 1995), the unpredictable behaviour of many impure salts of atmospheric interest near the crystallization point, the unknown ionic composition of the solute, and due to the presence of insoluble matter. Several studies have pointed out the widespread presence of water-insoluble material in urban aerosols (McMurry and Stolzenburg, 1989; Okada, 1985). By naming the water-insoluble mass fraction of the "dry" aerosol as δ, and the growth rate for the soluble part of the aerosol as $G(RH) = M_{wet}(RH)/M_{dry}$, the dry mass concentration is

$$M_{dry} = \frac{M_{wet}(RH)}{\delta + (1-\delta)\,G(RH)}. \quad (9)$$

For low RH, $M_{wet} \approx M_{dry}$ regardless of the value of δ. When RH is close to 100%, a relative underestimation δ of the dry mass occurs when considering, in the simulations, the wet aerosol to be fully soluble. In order to consider a possible presence of 0–50% insoluble matter in the dry aerosol, we calculated the minimum and maximum dry-mass concentrations as follows:

$$M_{dry\,mass} = \frac{M_{wet\,max}}{G(RH)}, \quad (10)$$

$$M_{dry\,min} = \frac{M_{wet\,min}}{0.5 + 0.5\,G(RH)}. \quad (11)$$

Results of the scattering simulations showed several points of interest for the interpretation of 532–1064 nm LIDAR data in terms of aerosol mass:

(a) CM_{532} showed an uncertainty of $<30\%$ for $70\% < RH < 98\%$ and $\alpha > 0.6$. In this range, the composition of the soluble part of the aerosol was quite unimportant, as was its absorption coefficient. This result was due to the considerable water dilution experienced by the aerosols, the refractive index of which became close to that of pure water as RH increased. For $RH < 70\%$, the aerosol was almost "dry", and its composition became very important in determining the optical properties. The choice of the aerosol model became critical (and often arbitrary) in this case. With $\alpha < 0.6$, the particle mode radius was around 1 μm or larger, and in this condition the 532–1064 nm LIDAR became size-insensitive, thus producing large errors in the estimation of the aerosol mass.

(b) The largest M_{wet} errors (up to 50%) were expected in the case of strongly absorbing and/or irregularly shaped coarse aerosols. This was the case of sooty aerosols or iron-rich dust. The largest uncertainties occurred for $RH < 80\%$.

(c) The resulted uncertainty on M_{dry} was always larger than that on M_{wet}.

According to these simulation results, LIDAR-derived mass data obtained with $RH > 98\%$, or $\alpha < 0.5$, or $\beta_{s,\lambda}(z_l) < 0.2\beta_{m,\lambda}(z_l)$ were deleted because they were expected to be unreliable. The LIDAR data obtained during rain events were not used. Processed LIDAR data were stored either as time–height–backscatter matrices for graphical purposes, or as monthly time series of M_{dry}, M_{wet}, and α.

2.4. Estimation of the aerosol backscatter scaling height

Assuming that the aerosol concentration near the ground decreases exponentially with altitude with a scaling height H (Pruppacher and Klett, 1978), and neglecting molecular backscatter and aerosol extinction, we have

$$V_\lambda(z) \propto \frac{e^{-z/H}}{z^2}, \tag{12}$$

H could be easily calculated from the derivative of the logarithm of $V'_\lambda(z)$, but when considering the LIDAR signal close to the ground, the uncertainty of the reference height, $z = 0$, in the LIDAR signal must be considered. Naming z_0 the absolute error in determining the $z = 0$ position in the LIDAR signal, the square-range corrected LIDAR signal becomes in fact

$$\beta_{a,\lambda}(z) \propto V'_\lambda(z) \propto \frac{(z - z_0)^2}{z^2} e^{-z/H} \approx e^{-z/H'}. \tag{13}$$

Close to the ground, the backscatter profile is thus deformed when z_0 is non-null.

The derivative of the logarithm of this deformed profile is

$$\frac{1}{H'} = \frac{d}{dz} \log(\beta_{a,\lambda}(z)) = -\frac{1}{H} + 2\frac{z_0}{z^2(1 - z_0/z)}, \tag{14}$$

H' converges to H for $z_0/z \to 0$, but could be significantly different in other cases. By assuming a maximum, systematic uncertainty $|z_0| = 10$ m due to electronics, simulations have shown that $H' \approx H$ within an error of 15% when $H < 100$ m and $z > 100$ m. In these conditions, H can be estimated with good approximation from $1/H = d\{\log[\beta_{a,\lambda}(z)]\}/dz$. H was thus estimated by fitting the profile of $\log[\beta_{a,1064}(z)]$ with a linear function between 100 and 500 m above the ground. In the low PBL, the exponential decreasing of backscatter with altitude is not a rule, as in some cases the backscatter profile was found to be quite flat with height in stable layers (usually in the early morning), or increased with height in the presence of cloudy layers. H should thus be considered to be just a rough estimator of the vertical profile. It should be also noted that H was measured at a height above 100 m, and thus the H values observed are not necessarily representative of the aerosol distribution just above the ground.

2.5. PBL-meteorology and pollution in Florence

Florence is located in a shallow valley of the Arno river, surrounded by hills (~500 m in altitude). The valley is about 60 m a.s.l., oriented in a SE–NW direction (Fig. 1). In a typical anticyclonic situation, prevailing winds come from the SE (from down town Florence) during nighttime, and from the W–NW (from the suburbs of Florence and the countryside) during daytime. Florence aerosols are mainly produced by civil combustion and by the rural areas surrounding the town. The sea is about 80 km away, and contributes to the aerosol budged mostly during frontal events. The LIDAR site is located in the western suburbs of Florence; thus, the diurnal westerly wind brings relatively clean air over the LIDAR, while the nocturnal SE winds push the polluted urban plume above the LIDAR.

Pollution and traffic data were collected from Agenzia Regionale per la Protezione Ambientale Toscana (ARPAT). These consisted of hourly chemical data from ground-based stations located in 14 sites in Florence, and daily averaged PM_{10} gravimetric data from 3 stations. Chemical data from the Via di Novoli station (located <1 km away from the LIDAR site), PM_{10} and hourly traffic data from the Via Ponte alle Mosse ARPAT station were used in this study.

3. Results

3.1. Daily aerosol cycles in summer

A typical anticyclonic summer LIDAR day is shown in Fig. 2. The time–altitude evolution of the backscatter is reported, showing an aerosol increase a few hours after dawn, in coincidence with the morning rush hours. A rapid aerosol depletion occurs in the late morning, in coincidence with the reversal of the wind direction and the increased wind speed. The wind reversal is accompanied by a development of the mixed layer (ML) (Stull, 1988) that breaks the stable nocturnal layer and dilutes vertically the pollutants. In Fig. 2, the PBL top is marked by clouds or by a sharp aerosol gradient: the PBL height increases markedly upto 1000–1500 m during the daytime because of the ML formation, and decreased again after dawn. During daytime, RH decreases due to the coupled effect of the temperature increase and of the advection of dry air from the countryside. Near the ground, α shows a maximum in the morning, revealing the accumulation of submicron-sized combustion aerosols in the low PBL during the early formation of the ML.

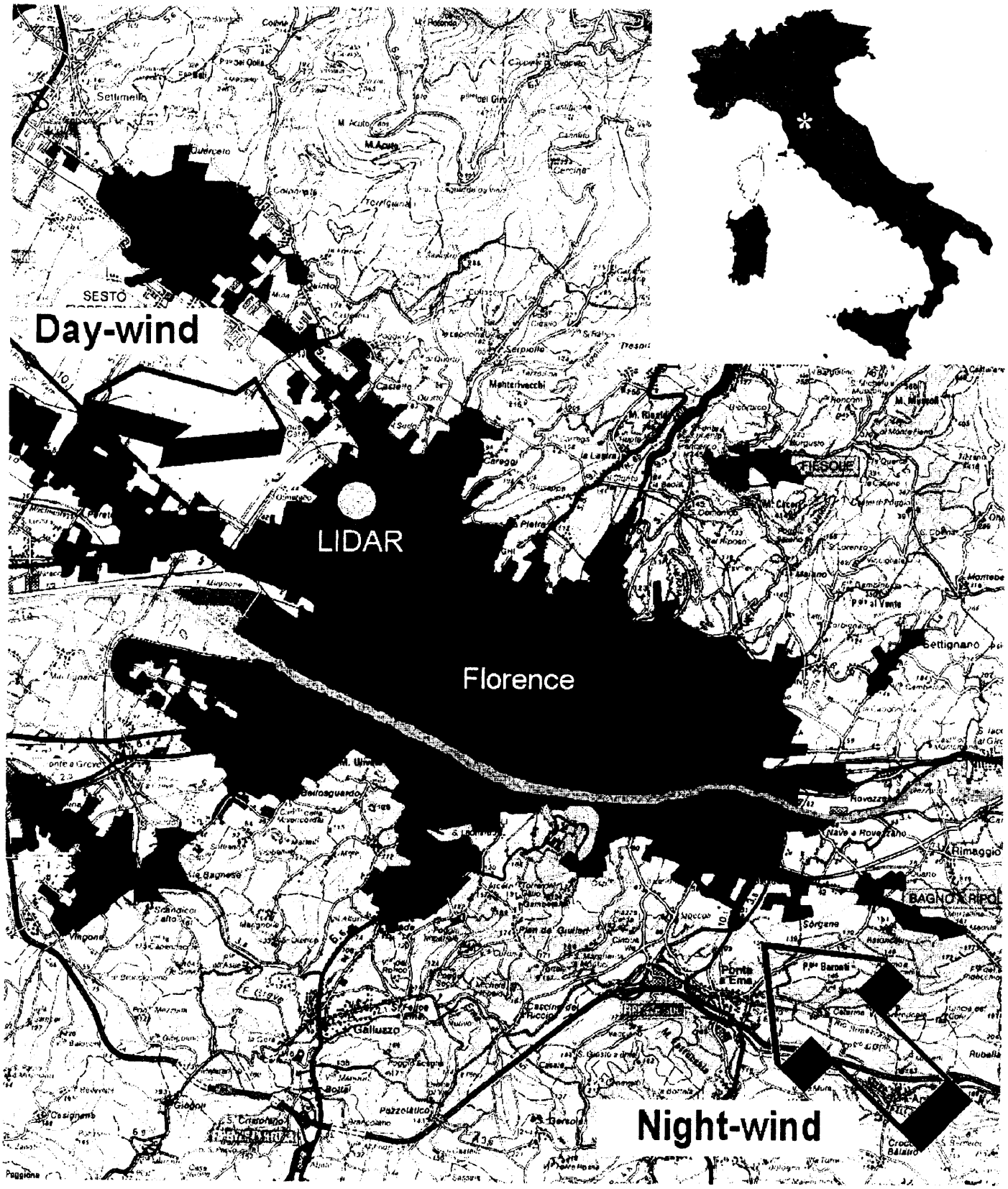

Fig. 1. Sketch of the study area. The position of the LIDAR and summer breeze-winds are evidenced.

The daily cycle of Fig. 2 was found to be a stable summer pattern in Florence, with the exception of rainy and windy days. In Fig. 3, the cyclic behaviour of α is reported for the whole month of August 2000. The daily pattern of α does not follow the traffic cycle: only the morning traffic peak is represented in the α data. The absence of the afternoon traffic peak is also evident in the NO_x data, which shows a quite good correlation

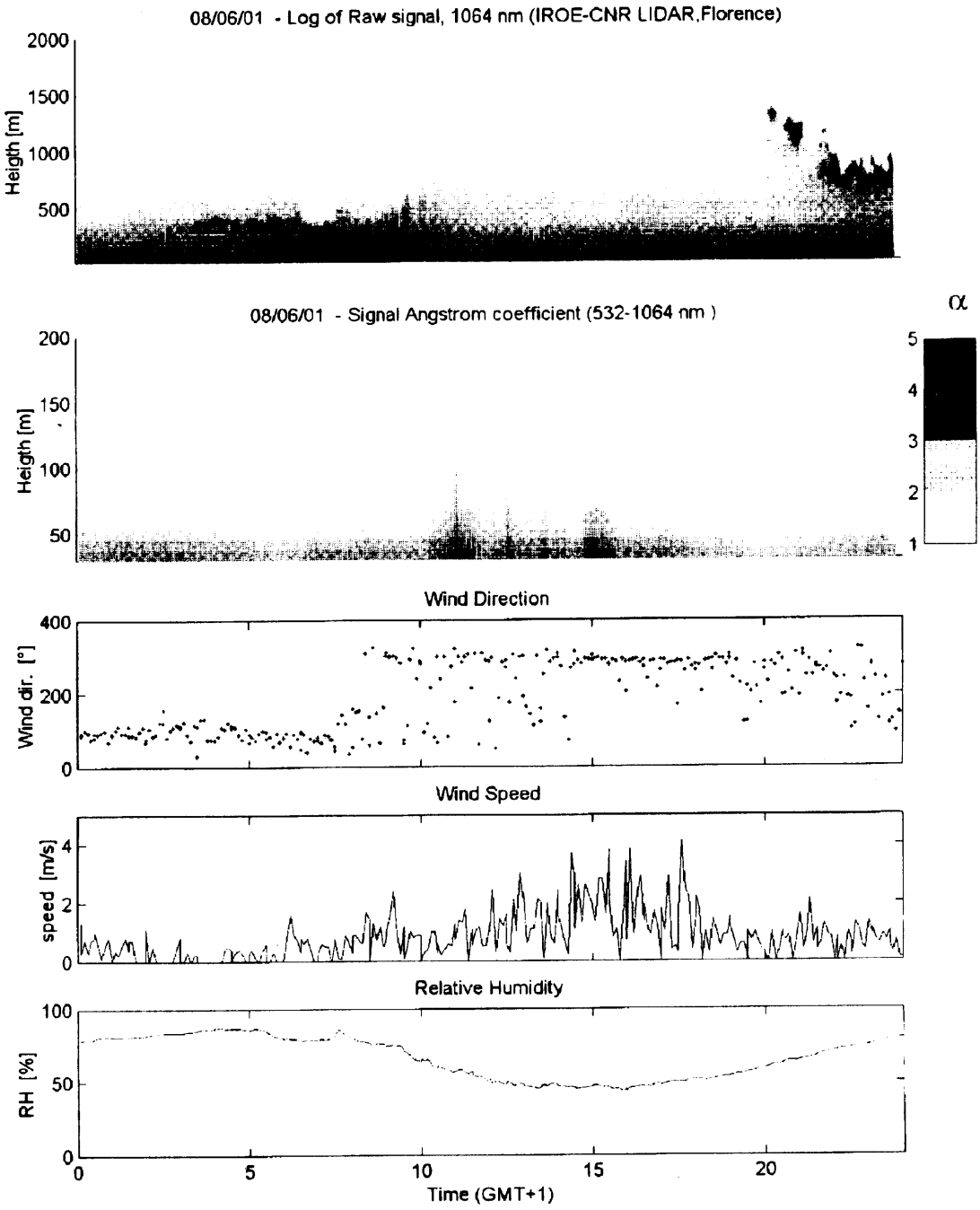

Fig. 2. LIDAR and meteo-data of a typical anticyclonic summer day (August 2001).

with α. Even if the aerosol size estimation by means of the 532–1064 nm LIDAR was affected by large uncertainties, the size ranges corresponding to α values have nonetheless been reported in Fig. 3. These indicative diameters were obtained for monomodal distributions of urban aerosols of differing natures and for 50% < RH < 95% (Del Guasta and Marini, 2000). A maximum value for α was evident for the whole period around 10 a.m. (GMT + 1) corresponding to dry particles of 0.04–0.1 μm median diameter. Size distributions from direct car emissions (Maricq et al., 1998; Harris and Maricq, 2001) showed maximum aerosol concentrations for particle diameters in the 0.04–0.07 μm range. Similar results were found in street canyons (Li et al., 1993). Recent works carried out at the roadside showed size distributions peaked at diameters even smaller that 0.04 μm, perhaps due to the formation of new particles from the gas phase (Harrison et al., 1999; Wehner et al., 2002). All these works showed that fresh urban aerosols contain a much larger proportion of ultrafine particles than does the background air. As urban aerosols are transported in the urban plume,

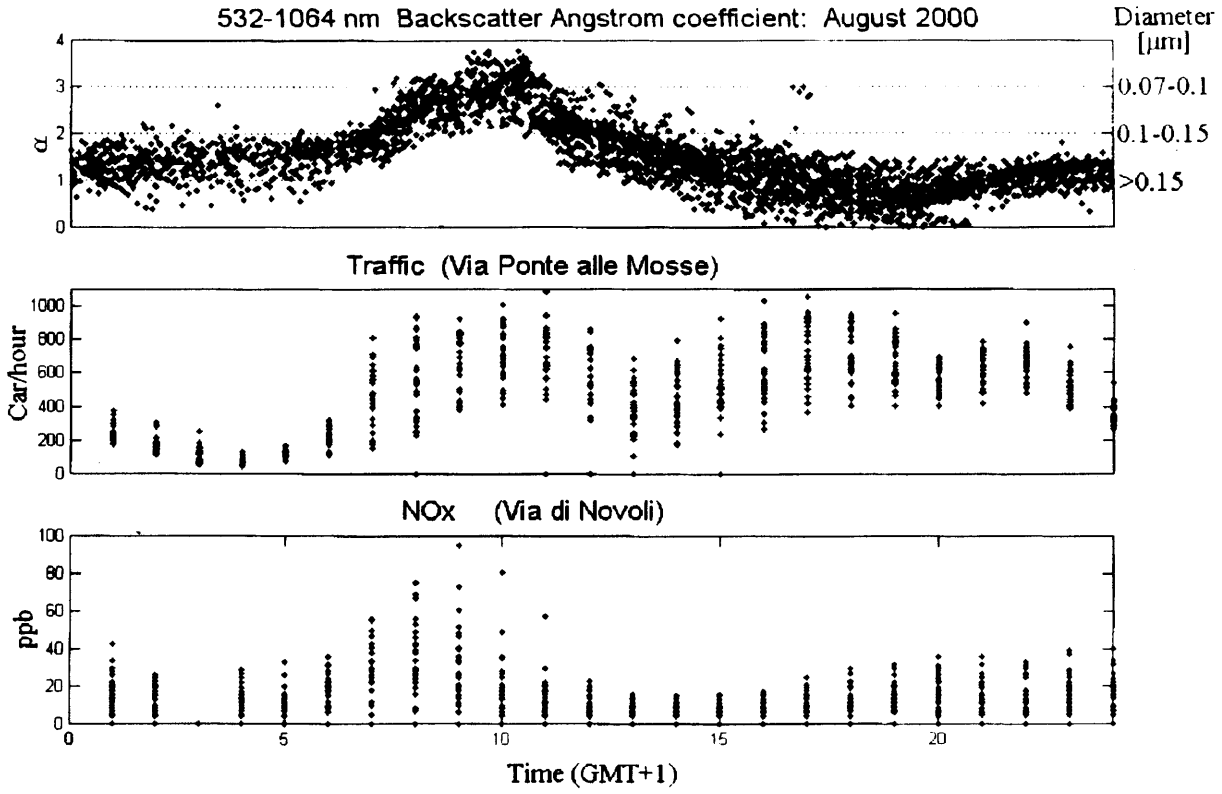

Fig. 3. The daily cycle of Ångström coefficient α in August 1998 compared with Traffic and NO_x cycles. The aerosol size corresponding to α is reported.

several processes (coagulation, condensational growth, vertical mixing with background aerosols, etc. (Turco and Yu, 1999)) lead to a reduced importance of the ultrafine component compared with the accumulation-mode. The mixing of urban air with rural air in the turbulent PBL also increases the median aerosol diameter by introducing a coarse aerosol mode. The LIDAR is particularly sensitive to these effects, because α decreases rapidly from 3–4 down to 1 with an increase in the median diameter from 0.02 to 0.1–0.5 μm (Del Guasta and Marini, 2000). For these reasons, the morning peak in α values observed in Florence can be considered to be a marker of fresh and fine urban aerosols, while the afternoon α values (0–1 range) is indicative of rural and/or aged urban aerosols. The afternoon α minimum could be explained with the presence of aerosols with a median size larger than about 0.1–0.15 μm. In the absence of direct measurements of the size distribution, this relatively large size could be achieved with the introduction of coarse aerosols (rural, aged urban) from sources located west of Florence and by the simultaneous moving away of fresh urban aerosols from the LIDAR due to the eastward wind direction. The enhanced surface-wind speed observed in the summer afternoons was likely to increase the concentration of coarse particles produced by erosion. A similar cycle in particle size and composition was observed by Kuhlbusch and Fissan (2001) in a rural area influenced by a town, on the basis of PM_x and black-carbon (BC) measurements. These authors observed an afternoon minimum of aerosols of urban origin and a corresponding increase in particle size, and indicated the daily wind cycle as being responsible for this feature.

The afternoon minimum in α was observed only in July and August: in the rest of the summer, α did not show a negative peak in the afternoon, and only the morning, positive peak was observed. This fact could be due to the strongly reduced traffic in Florence in July, August because of the summer holidays, coupled with an enhanced erosion occurring in the countryside due to the very dry summer.

The relative constancy of α throughout the night indicates both the absence of important traffic sources, and the fact that no significant aerosol growth occurred due to water uptake or coagulation. This is consistent with the limited span of RH values during the summer nights (Fig. 4), which rarely approached saturation: in these conditions, the maximum nighttime growth of the aerosol diameter was expected to be 10–15% (for RH passing from 80% to 90%) by assuming fully hygroscopic, $(NH_4)_2SO_4$ aerosols. The growth was smaller if we consider the widespread presence of insoluble matter in urban aerosols. For particles of a 0.1–0.15 μm median diameter, such a size increase would result in a change in α of the order of −0.15, a figure that is much smaller than the experimental uncertainties.

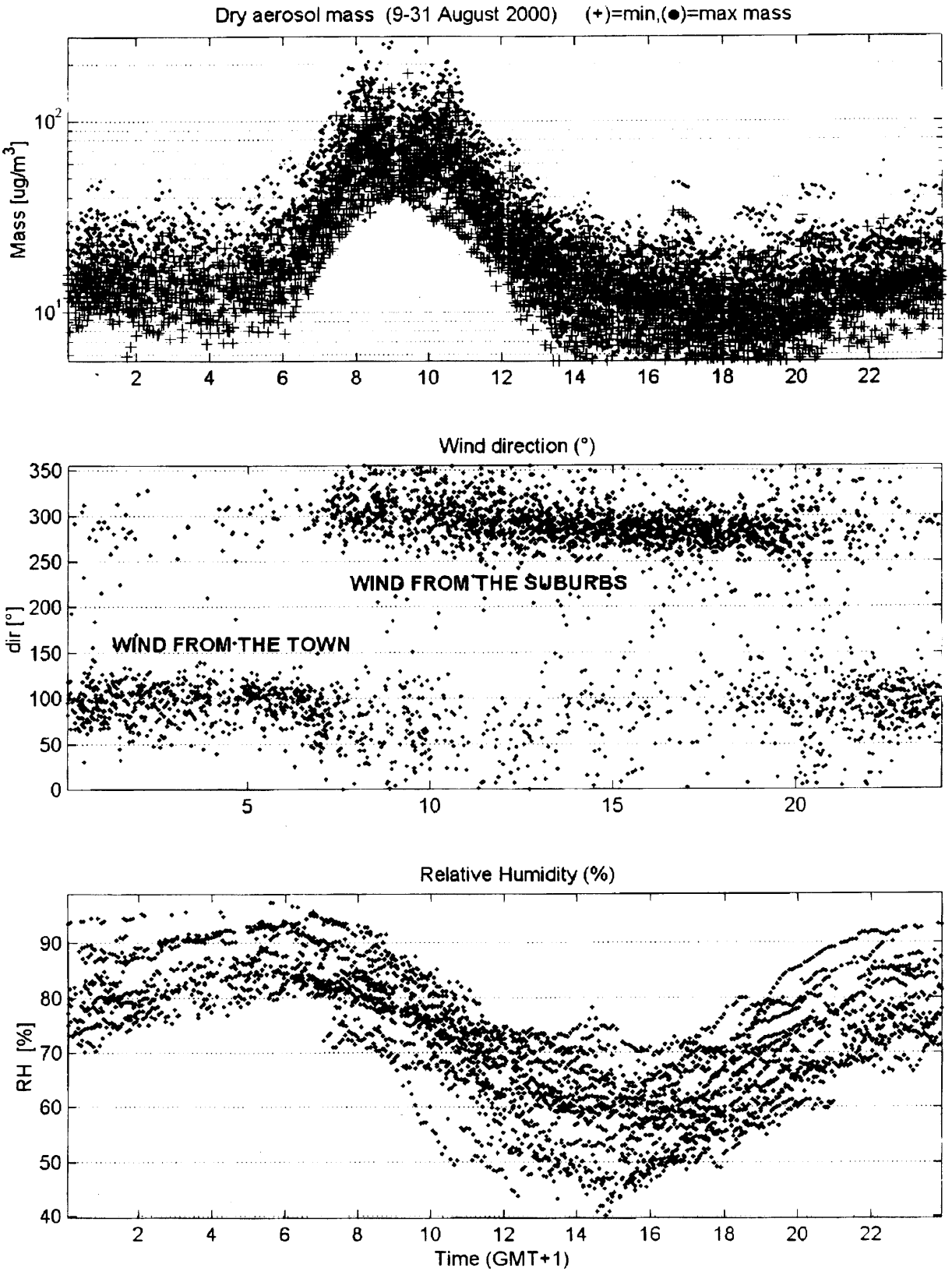

Fig. 4. The daily cycle of aerosol mass in August 2000. (+) minimum dry mass (averaged value 20 $\mu g\,m^{-3}$). (•) maximum dry mass (averaged value 29 $\mu g\,m^{-3}$). The wind and RH cycle are also shown.

Fig. 4 the cyclic behaviour of the dry aerosol mass is reported for August 2000. A clean daily cycle is evident, with a peak in the late morning, that is out of phase with RH. A very similar result (but with a less pronounced morning peak) was obtained by Harrison et al. (1999), and Wehner and Wiedensohler (2000) by using aerosol

samplers. It should be noted that the peak mass concentration was almost 5–10 times higher than the daily averaged concentration (that was assimilable to the quantity usually measured in ground-based networks such as PM_{10}). Even if part of this large difference could be due to an improper optical modelling of the aerosols, the mass peak should be considered when estimating the PM_{10} exposition of people in epidemiological studies on the basis of standard measurements.

3.2. *Summer correlation between aerosol mass and traffic cycles*

The reversal in the wind direction in Florence on a typical summer day makes it evident that no simple correlation can be found between the LIDAR-derived aerosol mass time series and that of the traffic. In the morning, the advection of urban air above the LIDAR site makes such a correlation possible, but the mass concentration in the afternoon hours is related to distant sources, and the mass concentration is more related to a regional "background" than to metropolitan sources. Also, the mass concentration in the morning is the sum of a regional "background" (that changes with the synoptic conditions) and a local contribution approximately in phase with the local sources. This situation is depicted in Fig. 5 for the July–August 1998 period.

It is evident that the reduced traffic of the weekends did not correspond to a reduced aerosol mass, showing that source variations in the time scale of 1–2 days are smoothed out in the aerosol pattern of Florence. Also, only one of the two daily traffic peaks is represented in the aerosol time series, a summer feature observed also by Wehner and Wiedensohler (2000). A good correlation between traffic and aerosol mass derived from the LIDAR was obtained by selecting the conditions in which the LIDAR was downwind with respect to the town, the wind was moderate (speed $< 3\,m\,s^{-1}$), and the envelope of the nighttime minimum mass, that could be assimilated to the regional background, was subtracted from the mass time series. The result is shown in

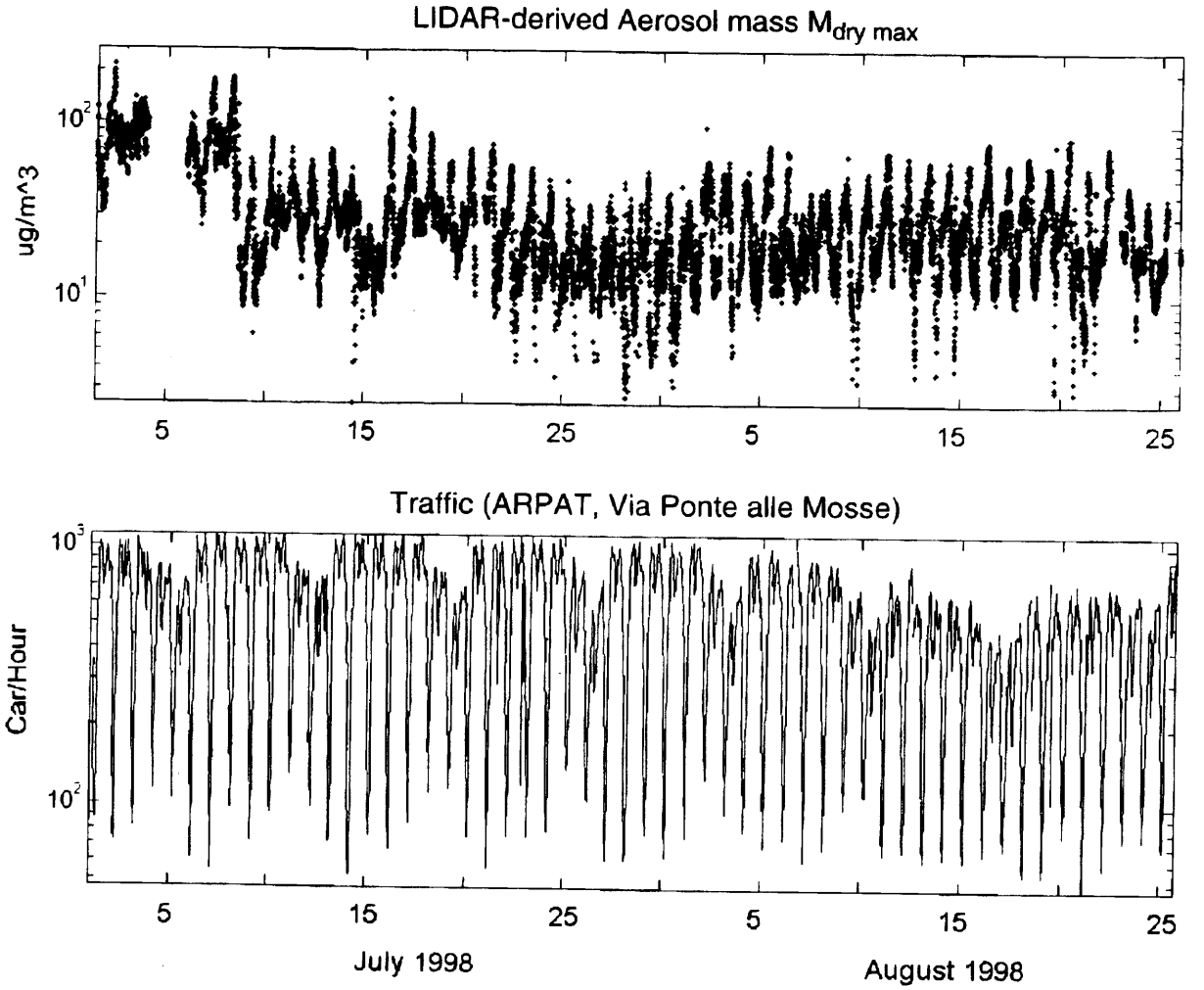

Fig. 5. Comparison of the time series of (maximum) dry aerosol mass concentration and traffic for July–August 1998.

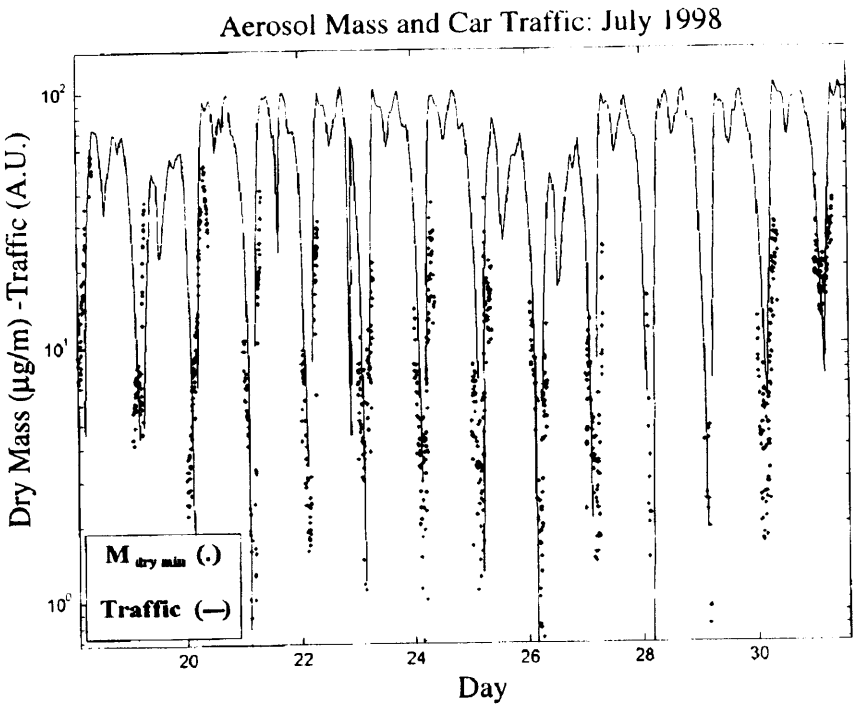

Fig. 6. Comparison of dry aerosol mass and traffic for 14 days in July 1998. The low-frequency regional background was subtracted from the aerosol mass time series.

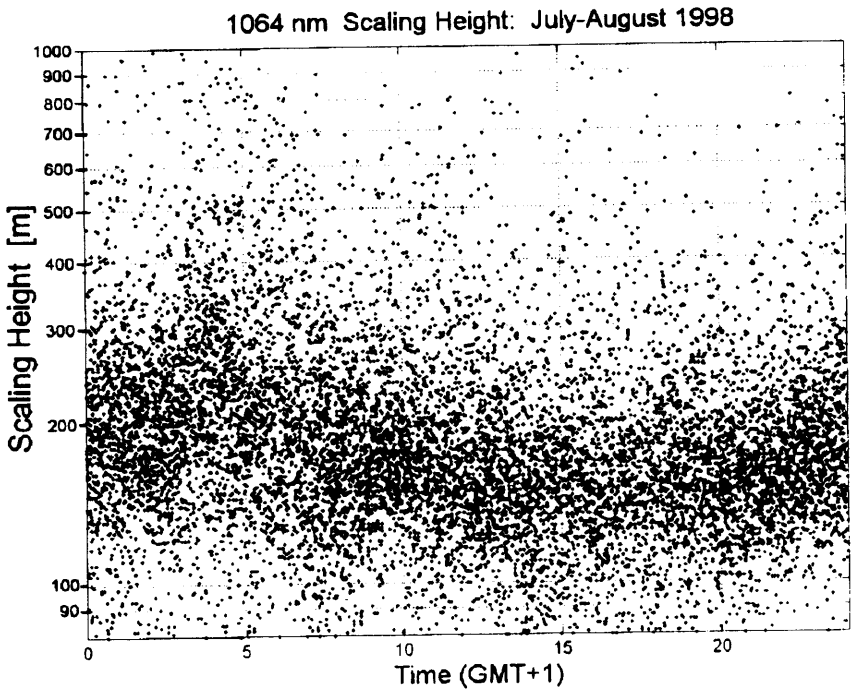

Fig. 7. Summer cycle of the aerosol backscatter scale-height H, as computed between 100 and 500 m above the ground (see text).

Fig. 6 for 14 days of measurements. The aerosol mass variations (5 min resolution) followed faithfully the traffic variations (1 h resolution) without any evident phase shift. This is a further demonstration that the morning α peak can be considered as a marker of the presence of fresh traffic aerosols.

3.3. Aerosol scaling height cycle in summer

In the summer months, a cyclic behaviour of the aerosol backscatter scaling height was evidenced (Fig. 7). The cycle was less "clean" than those of the aerosol mass and Ångström coefficient because of the

wide variability in vertical aerosol structures, especially in stable nocturnal conditions. The maximum H values were measured during the first hours of the morning, when the backscatter in the lower PBL was vertically homogeneous due to the atmospheric stability and to the absence of significant sources of aerosol. Between 4 and 6 a.m., in coincidence with the maximum RH, H showed wide day-to-day fluctuations, due to the formation of foggy stratifications through water uptake. Around 6 a.m. the traffic introduced aerosols in the SL at ground level. H decreased significantly down to ~150–200 m, and fluctuations were reduced. In the late morning and in the afternoon, the horizontal advection of dry suburban air resulted in small H values that were usually in the 100–200 m range. The relatively short-scaling height observed in the afternoon was in contrast with the presence of a well-developed mixed layer (the vertical extent of the ML was often revealed by the presence of clouds at its top, as in Fig. 2). The RH at ground level was so low (50–70%) at that time of the day that the vertical backscatter gradient could not be due to a differential hygroscopic growth in the urban aerosols with height. In the absence of balloon soundings, this gradient could be explained with the low-altitude, horizontal transport of relatively coarse particles from the countryside on the part of the enhanced surface-winds.

4. Conclusions

The quasi-periodical evolution of aerosol mass as shown in this work resulted a typical feature of the summer months in Florence. In winter and spring the ML formation is often inhibited by the low radiation on the ground, coupled with the presence of fog layers and a thermal inversion in the first 100–300 m above the ground. No evident correlation between LIDAR-derived aerosol mass and traffic was observed on a regular basis in winter. This result is partly due to the relevant presence of domestic-heating aerosols in winter (a presence that masks the high-frequency signal of car emissions), and partly due to the high variability in meteorological conditions, with stagnation events alternating with days of strong, dry northerly winds or weak and humid southern winds. Also, the usually high RH values and the fog/rain events observed in winter reduced the number of LIDAR data valid for an estimation of the aerosol mass and scaling height. Summer, on the other side, resulted in an ideal playground for LIDAR investigations in Florence, due to the relatively low RH and due to the quasi-periodic behaviour of the PBL meteorology and aerosol optical properties. Daily cycles of the aerosol mass and of the backscatter Ångström coefficient were clearly identified and correlated with the traffic and meteorological cycles. The observed cycles showed the daily alternation of fine, fresh urban aerosol with larger, rural aerosols at the LIDAR site, located at the western periphery of the town. LIDAR evidenced a sharp aerosol mass peak due to very fine particles produced as primary aerosols by car traffic. The peak occurrs during the morning rush hours, when most people are breathing outdoor air. In view of the increasing awareness concerning the health risks of fine and ultrafine urban aerosols, this result suggest a refinement of the aerosol instruments and measurement networks operating at present in Florence, in order to achieve a time resolution of aerosol mass measurements of at least one hour. Even if the automatic LIDAR was shown to be a promising tool for the unattended monitoring of urban aerosols, validation studies involving in situ aerosol samplers will be necessary in order to validate the LIDAR-derived mass concentrations. This is of particular importance because, at the present moment, derivation of the suspended mass from LIDAR data necessarily relies on a comprehensive aerosol model that is probably inadequate for a local study. In particular, some size- and time-resolved optical properties (complex refractive index) and chemical properties (insoluble content, growth factor) of urban aerosols are definitely required.

Acknowledgements

The author wishes to acknowledge the support of the Programma Nazionale di Ricerche in Antartide (PNRA), which supported the development of the automatic LIDAR; the "Agenzia Regionale per la Protezione Ambientale della Toscana" (ARPAT) for the traffic and pollution data used in this paper; Stefano Balestri, Francesco Castagnoli, Marco Morandi, and Valerio Venturi for the design and implementation of the PBL–LIDAR prototype.

References

Ackermann, J., 1998. The extinction-to-backscatter ratio of tropospheric aerosols: a numerical study. Journal of Atmospheric and Oceanic Technology 15, 1043–1050.

Anderson, T.L., Masonis, S.J., Covert, D.S., Charlson, R.J., Rood, M.J., 2000. In situ measurement of the aerosol extinction-to-backscatter ratio at a polluted continental site. Journal of Geophysical Research 105, 26907–26915.

Collis, R.T.H., Russel, P.B., 1976. Lidar measurement of particles and gases by elastic backscattering and differential absorption. In: Hinkley, E.D. (Ed.), Laser Monitoring of the Atmosphere. Springer, Berlin, pp. 71–151.

Del Guasta, M., Venturi, V., 1998. Dispositivo a semiconduttore per la misura dell'energia del singolo sparo di laser Nd-YAG impulsati. Technical report IROE TR/ATM/01.98, pp. 11.

Del Guasta, M., Marini, S., 2000. On the retrieval of urban aerosol mass concentration by a 532 and 1064 nm LIDAR. Journal of Aerosol Science 31, 1469–1488.

Devara, P.C.S., Raj, P.E., Sharma, S., 1994. Remote sensing of atmospheric aerosol in the nocturnal boundary layer. Environmental Pollution 85, 97–102.

Di Girolamo, P., Ambrico, P.F., Amodeo, A., Borselli, A., Pappalardo, G., Spinelli, N., 1999. Aerosol observations by lidar in the nocturnal boundary layer. Applied Optics 38, 4585-4595.

Harris, J.S., Maricq, M.M., 2001. Signature size distributions for diesel and gasoline engine exaust particulate matter. Journal of Aerosol Science 32, 749–764.

Harrison, R.M., Jones, M., Collins, G., 1999. Measurements of the physical properties of particles in the urban atmosphere. Atmospheric Environment 33, 309–321.

Kent, G.S., 1978. Deduction of aerosol concentrations from 1.06-im lidar measurements. Applied Optics 12, 3763–3773.

Klett, A.D., 1981. Stable analytical solution for processing LIDAR returns. Applied Optics 20, 211–220.

Kuhlbusch, J.A.C., Fissan, H., 2001. Diurnal variations of particle characteristics at a rural measuring site close to the Ruhr-area, Deutschland. Atmosheric Environment 35, S13–S21.

Li, C.-S., Lin, W.-H., Jenq, F.-T., 1993. Characterization of outdoor submicron particles and selected combustion sources of indoor particles. Atmospheric Environment 27B, 413–429.

Li, C.-S., Lin, W.-H., Jenq, F.-T., 1993. Characterization of outdoor submicron particles and selected combustion sources of indoor particles. Atmospheric Environment 27B, 413–424.

Maricq, M.M., Podsiadlik, D.H., Chase, R.E., 1998. Gasoline vehicle patrticle size distributions: comparison of steady state, FTP and US06 measurements. Environmental Science and Technology 32, 2033–2042.

McMurry, P.H., Stolzenburg, M., 1989. On the sensitivity of particle size to relative humidity for Los Angeles aerosols. Atmospheric Environment 23, 497–507.

Measures, R.M., 1988. Laser Remote Chemical Analysis, Wiley, New York, p. 49.

Menut, L., Flamant, C., Pelon, J., Valentin, R., Flamant, P.H., Dupont, E., Carissimo, B., 1997. Study of the boundary layer structure over the Paris agglomeration as observed during the ECLAP experiment. In: Ansmann, A., Neuber, R., Rairoux, P., Wandinger, U. (Eds.), Advances in Atmospheric Remote Sensing with LIDAR. Springer, Berlin, pp. 15–18.

Okada, K., 1985. Number-size distribution and formation process of submicrometer sulfate-containing particles in the urban atmosphere of Nagoya. Atmospheric Environment 19, 743–757.

Penndorf, R., 1957. Tables of the refractive index for standard air and the Rayleigh scattering coefficient for the spectral region between 0.2 and 20 μm and their application to atmospheric optics. Journal of the Optical Society of America 47 (2), 176–182.

Pinnick, R.G., Jennings, S.G., Chylek, P., Ham, C., Grandy, W.T., 1983. Backscatter and extinction in water clouds. Journal of Geophysical Research 88, 6787–6796.

Pradeep, S., Hindelmann, L.M., McMurry, P.H., Seinfeld, J.H., 1995. Organics alter hygroscopic behaviour of atmospheric particles. Journal of Geophysical Research 100, 18755–18770.

Pruppacher, H.R., Klett, J.D. 1978. Microphysics of Clouds and Precipitation, Reidel, Dordrecht, p. 713.

Shettle, E.P., Fenn, R.W., 1979. Models for the aerosols of the lower atmosphere and the effects of humidity variations on their optical properties, Air Force Geophysics Laboratory, Hamscom, Environmental Research Papers 676, p. 94.

Stull, R.B., 1988. An Introduction to Boundary Layer Meteorology, Kluwer Academic Publishers, Dordrecht, p. 666.

Turco, R.P., Yu, F., 1999. Particle size distribution in an expanding plume undergoing simultaneous coagulation and condensation. Journal of Geophysical Research 104, 19227–19241.

Wehner, B., Wiedensohler, A., 2000. Seasonal and diurnal variability of the PM_{10} mass concentration in the urban area of Leipzig, Germany. Journal of Aerosol Science 31 (Suppl. 1), 566–567.

Wehner, B., Birmili, W., Gnauck, T., Wiedensohler, A., 2002. Particle number size distributions in a street canyon and their transformation into the urban-air background: measurements and a simple model study. Atmospheric Environment 36 (13), 2215–2223.

Willeke, K., Baron, P.A., 1993. Aerosol Measurement, Van Nostrand Reinhold, New York, p. 310.